16èmes Journées Internationales de Thermique (JITH 2013)
Marrakech (Maroc), du 13 au 15 Novembre, 2013

Conjugate Heat Transfer in an Annular Duct Equipped with Heat Generating Fins

Sofiane TOUAHRI, Toufik BOUFENDI
Energy Physics Laboratory, Physics Department, Faculty of Sciences
University of Constantine 1, 25000, Algeria
sofianetouahri04@yahoo.fr; ***boufendit@yahoo.fr***

Abstract: In this work, we numerically study the three-dimensional conjugate mixed convection heat transfer in a horizontal annulus equipped by longitudinal attached fins on internal surface of outer cylinder. The external pipe and the fins are heated by an electrical current passing through their small thickness. The number of longitudinal fins studied is: 2 vertical, 4 and 8 fins. The convection in the fluid domain is conjugated to thermal conduction in the pipes and fins solid thickness. The physical properties of the fluid are thermal dependant. The heat losses from the external pipe surface to the surrounding ambient are considered. The model equations of continuity, momenta and energy are numerically solved by a finite volume method with a second order spatiotemporal discretization. The obtained results showed that the axial Nusselt number increases with the increasing of number and height of fins. The participation of fins located in the lower part of the tube on the improvement of heat transfer is higher than the participation of the upper fins.

Keywords: Conjugate Heat Transfer; Mixed Convection; Internal Fins; Numerical simulation.

1. Introduction

Finned tubes are often used in many engineering sectors for extend the contact surface between the tube wall and the fluid and improve the heat transfer; the researchers have studied the problem of optimizing the shape and geometry of attached fins in order to increase heat transfer effectiveness. Many investigations, both experimental and numerical, have been conducted for different kinds of internally finned tubes. Patankar et al.[1], presented an analytical model for fully developed turbulent air flow in internally finned tubes and annuli. In their study, the longitudinal attached fins in the inner wall were considered. With thermal boundary conditions such the constant heat flux at the inner surface, the results of this study concerns the heat transfer and the pressure drop coefficients. The obtained results are presented as determining the Nusselt numbers and coefficients of charge loss. Agrawal et al.[2], studied numerically the effect of varying the geometric parameters and the Reynolds number on the pressure drop and the heat transfer. This study was conducted for the case of longitudinal fins attached to the inside of an annulus. In the numerical work of Farinas et al. [3], the authors studied the laminar mixed convection in an annulus with inner fins for two, four and sixteen fins. The inner wall is hot while the outer wall is cold. The Grashof number varied from 10^2 to 10^4. The conservation equations are solved by the finite difference method. The results are presented for the air with Rayleigh numbers varied from 10^3 to 10^6 for different configurations of fins (fine, rounded or divergent) and different lengths of blades (L = 0.25, 0,5 and 0,75). The results are presented as isotherms graphs, velocity fields and the variation of Nusselt numbers. The heat transfer is enhanced to a rounded configuration of the fins. Similar studies were also treated experimentally by Wei-Mon Yan et al. [4], B. Yu et al. [5] and Wang et al. [6].

In the present work, we have studied numerically the heat transfer by mixed convection in annulus between two concentric cylinders. Longitudinal fins are attached in the inner wall of the outer cylinder. The mixed convection is conjugated with the thermal conduction in the pipes and fins walls. The physical properties of the fluid are thermal-dependent and heat losses to the outside environment are taken into account while the inner cylinder is adiabatic at its inner wall. The objective of our work is to study the improvement of heat transfer in the annulus using 2, 4 and 8 longitudinal fins generating heat.

2. Mathematical Model

Figure 1 illustrates the geometry of the problem studied. Two long horizontal concentric cylinders having a length L=1m, the inner tube with an internal diameter D_{1i}=0.46 cm and an outer diameter D_{1o}=0.5 cm, while the outer tube with an internal diameter D_{2i}=0.96 cm and an outer diameter D_{2o}=1 cm. Longitudinal fins are attached to the inner wall of the outer cylinder. At the entrance, the flow has an average axial velocity equal to 9.88 10^{-2} m/s and a constant temperature of 15 °C.

The Reynolds and the Prandtl numbers are equal to 399.02 and 8.082 respectively. The non-dimensional fluid viscosity and thermal conductivity variations with temperature are represented by the functions $\mu^*(T^*)$ and $K^*(T^*)$ obtained by smooth fittings of the tabulated values cited by Baehr and Stephan [7].

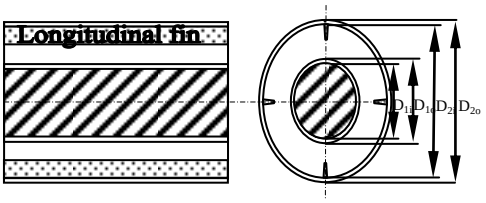

Figure 1: Geometry of the Problem

2.1. Modelling Equations

2.1.1. Mass Conservation Equation

$$\frac{1}{r^*}\frac{\partial}{\partial r^*}\left(r^* V_r^*\right)+\frac{1}{r^*}\frac{\partial V_\theta^*}{\partial \theta}+\frac{\partial V_z^*}{\partial z^*}=0 \tag{1}$$

2.1.2. Radial Momentum Conservation Equation

$$\frac{\partial V_r^*}{\partial t^*}+\frac{1}{r^*}\frac{\partial}{\partial r^*}\left(r^* V_r^* V_r^*\right)+\frac{1}{r^*}\frac{\partial}{\partial \theta}\left(V_\theta^* V_r^*\right)+\frac{\partial}{\partial z^*}\left(V_z^* V_r^*\right)-\frac{V_\theta^{*2}}{r^*}= \tag{2}$$
$$-\frac{\partial P^*}{\partial r^*}+\frac{Gr_0^*}{\mathrm{Re}_0^2}\cos\theta\ T^*+\frac{1}{\mathrm{Re}_0}\left[\frac{1}{r^*}\frac{\partial}{\partial r^*}\left(r^*\tau_{rr}^*\right)+\frac{1}{r^*}\frac{\partial}{\partial \theta}\left(\tau_{r\theta}^*\right)-\frac{\tau_{\theta\theta}^*}{r^*}+\frac{\partial}{\partial z^*}\left(\tau_{rz}^*\right)\right]$$

2.1.3. Angular Momentum Conservation Equation

$$\frac{\partial V_\theta^*}{\partial t^*}+\frac{1}{r^*}\frac{\partial}{\partial r^*}\left(r^* V_r^* V_\theta^*\right)+\frac{1}{r^*}\frac{\partial}{\partial \theta}\left(V_\theta^* V_\theta^*\right)+\frac{\partial}{\partial z^*}\left(V_z^* V_\theta^*\right)+\frac{V_r^* V_\theta^*}{r^*}= \tag{3}$$
$$-\frac{1}{r^*}\frac{\partial P^*}{\partial \theta}-\frac{Gr_0^*}{Re_0^2}\sin\theta\ T^*+\frac{1}{Re_0}\left[\frac{1}{r^{*2}}\frac{\partial}{\partial r^*}\left(r^{*2}\tau_{\theta r}^*\right)+\frac{1}{r^*}\frac{\partial}{\partial \theta}\left(\tau_{\theta\theta}^*\right)+\frac{\partial}{\partial z^*}\left(\tau_{\theta z}^*\right)\right]$$

2.1.4. Axial Momentum Conservation Equation

$$\frac{\partial V_z^*}{\partial t^*}+\frac{1}{r^*}\frac{\partial}{\partial r^*}\left(r^* V_r^* V_z^*\right)+\frac{1}{r^*}\frac{\partial}{\partial \theta}\left(V_\theta^* V_z^*\right)+\frac{\partial}{\partial z^*}\left(V_z^* V_z^*\right)= \tag{4}$$
$$-\frac{\partial P^*}{\partial z^*}+\frac{1}{\mathrm{Re}_0}\left[\frac{1}{r^*}\frac{\partial}{\partial r^*}\left(r^*\tau_{rz}^*\right)+\frac{1}{r^*}\frac{\partial}{\partial \theta}\left(\tau_{\theta z}^*\right)+\frac{\partial}{\partial z^*}\left(\tau_{zz}^*\right)\right]$$

2.1.5. *Energy Conservation Equation*

$$\frac{\partial T^*}{\partial t^*}+\frac{1}{r^*}\frac{\partial}{\partial r^*}\left(r^* V_r^* T^*\right)+\frac{1}{r^*}\frac{\partial}{\partial \theta}\left(V_\theta^* T^*\right)+\frac{\partial}{\partial z^*}\left(V_z^* T^*\right)=G^*-\frac{1}{Re_0\,Pr_0}\left[\frac{1}{r^*}\frac{\partial}{\partial r^*}\left(r^* q_r^*\right)+\frac{1}{r^*}\frac{\partial}{\partial \theta}\left(q_\theta^*\right)+\frac{\partial}{\partial z^*}\left(q_z^*\right)\right] \tag{5}$$

$$\tau_{rr}^*=2\mu^*\frac{\partial V_r^*}{\partial r^*}\qquad \tau_{r\theta}^*=\tau_{\theta r}^*=\mu^*\left[r^*\frac{\partial}{\partial r^*}\left(\frac{V_\theta^*}{r^*}\right)+\frac{1}{r^*}\frac{\partial V_r^*}{\partial \theta}\right]\qquad \tau_{\theta\theta}^*=2\mu^*\left[\frac{1}{r^*}\frac{\partial V_\theta^*}{\partial \theta}+\frac{V_r^*}{r^*}\right] \tag{6}$$

$$\tau_{\theta z}^*=\tau_{z\theta}^*=\mu^*\left[\frac{\partial V_\theta^*}{\partial z^*}+\frac{1}{r^*}\frac{\partial V_z^*}{\partial \theta}\right]\qquad \tau_{zz}^*=2\mu^*\frac{\partial V_z^*}{\partial z^*}\qquad \tau_{zr}^*=\tau_{rz}^*=\mu^*\left[\frac{\partial V_z^*}{\partial r^*}+\frac{\partial V_r^*}{\partial z^*}\right]$$

$$q_r^*=-K^*\frac{\partial T^*}{\partial r^*},\qquad q_\theta^*=-\frac{K^*}{r^*}\frac{\partial T^*}{\partial \theta^*}\qquad et\qquad q_z^*=-K^*\frac{\partial T^*}{\partial z^*} \tag{7}$$

2.2. The boundary Conditions

2.2.1 At the Annulus Entrance : $Z^*=0$

In the Fluid Domain: $$V_r^*=V_\theta^*=T^*=0, V_z^*=1 \tag{8}$$

In the Solid Domain: $$V_r^*=V_\theta^*=V_z^*=T^*=0 \tag{9}$$

2.2.2 At the Annulus Exit : $Z^*=217.39$

In the Fluid Domain: $$\frac{\partial V_r^*}{\partial z^*}=\frac{\partial V_\theta^*}{\partial z^*}=\frac{\partial V_z^*}{\partial z^*}=\frac{\partial}{\partial z^*}\left(K^*\frac{\partial T^*}{\partial z^*}\right)=0 \tag{10}$$

In the Solid Domain: $$V_r^*=V_\theta^*=V_z^*=\frac{\partial}{\partial z^*}\left(K^*\frac{\partial T^*}{\partial z^*}\right)=0 \tag{11}$$

2.2.3 At the Inside Wall of Internal Pipe, $r^*=0.5$:

$$V_r^* = V_\theta^* = V_z^* = 0 \quad et \quad \frac{\partial T^*}{\partial r^*} = 0 \tag{12}$$

2.2.4 At the Outer Wall of External Pipe: $r^*=1.087$

$$\begin{cases} V_r^* = V_\theta^* = V_z^* = 0 \\ -K^* \dfrac{\partial T^*}{\partial r^*} = \dfrac{(h_r + h_c) D_i}{K_0} T^* \end{cases} \tag{13}$$

$$h_r = \varepsilon \sigma \left(T^2 + T_\infty^2\right)\left(T + T_\infty\right) \tag{14}$$

The emissivity of the outer wall ε is arbitrarily chosen to 0.9 while h_c is derived from the correlation of Churchill and Chu [8] valid for all Pr and for Rayleigh numbers in the range $10^{-6} \le Ra \le 10^9$.

$$Nu = [h_c \; D_i \; / K_{air}] = \left[0.6 + \left(0.387\, Ra^{1/6} \; / \left(1 + (0.559/\mathrm{Pr}_{air})^{9/16}\right)^{8/27}\right)\right]^2 \tag{15}$$

2.3. Nusselt Number

At the pipes wall interface ($r^*= r_{2i}^*=1.0435$) the local Nusselt number is defined as:

$$Nu\,(\theta, z^*) = \frac{h\,(\theta, z^*)\, D_i}{K_0} = \left[\frac{\left(K^* \partial T^* / \partial r^*\right)_{r^* = r_{2i}^*}}{T^*(0.5, \theta, z^*) - T_m^*(z^*)}\right] \tag{16}$$

At the fins wall interface ($\theta= \theta_{fin}$) the local Nusselt number is defined as:

$$Nu\,(r^*, z^*) = \frac{h\,(r^*, z^*)\, D_h}{K_0} = \left[\frac{\left(K^*/r^*\right)\left(\partial T^* / \partial \theta\right)\big|_{\theta = \theta_{fin}}}{T^*(r^*, \theta_{fin}, z^*) - T_m^*(z^*)}\right] \tag{17}$$

3. Numerical resolution

For the numerical solution of modelling equations, we used the finite volume method well described by Patankar [9]. The using of this method involves the discretization of the physical domain into a discrete domain constituted of finite volumes where the modelling equations are discretized in a typical volume. We used a temporal discretization with a truncation error of $\left(\Delta t^*\right)^2$ order. The mesh used contains 52×88×162 points in the radial, azimuthal and axial directions and the considered time step is $\Delta t^* = 5 \cdot 10^{-4}$. The steady state is controlled by the satisfaction of the global mass and energy balances as well as the leveling off of the time evolution of the hydrodynamic and thermal fields.

4. Results and discussion

All the results presented in this paper were calculated for Reynolds number, Re = 399.02, the Prandtl number, Pr = 8.082, the Grashof number is equal to 12801 while the fin height H^* is equal to 0.12. For the brevity of the paper, the results obtained for another fin height H^* (=0.24) are not presented.

4.1. Development of hydrodynamic flow

The obtained flow for the studied cases is characterized by a main flow along the axial direction and a secondary flow influenced by the density variation with temperature, which occurs in the plane *($r^* - \theta$).* These flows are presented for 8 longitudinal fins.

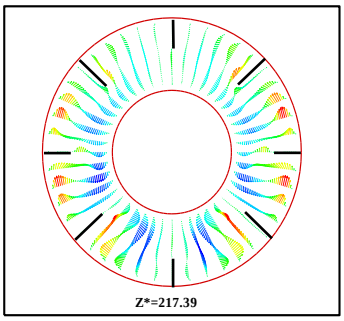

Figure 2: Development of the secondary flow at the annulus exit .

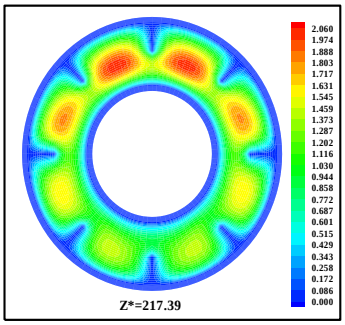

Figure 3: Axial velocity profile at the annulus exit.

In figure 2, we present the secondary flow vectors at the annulus exit (Z^*=217.39). The transverse flow is explained as follows: the hot fluid moves along the inner wall of the external cylinder from the bottom (θ=π) to the top (θ=0), this movement is blocked by the walls of the longitudinal fins. After, a portion of the fluid continues moving upwardly under the effect of the thermal buoyancy force while another part is conveyed downwardly with the relatively cold fluid which descends near of the inner cylinder. The transverse flow in the $(\overrightarrow{r^*},\theta)$ plane is represented by counter rotating cells; the cells number is proportional to longitudinal fins number used. The vertical plane passing through the angles $(\theta=0)$ and $(\theta=\pi)$ is a plane of symmetry. Regarding axial flow, this latter is influenced by the generation of the secondary flow which causes an angular variation explained as follows: the thermal viscosity is inversely proportional to the fluid temperature and the axial velocity increases with the decrease of viscosity, automatically we will have an axial velocity relatively high in the upper part of the annulus where the fluid temperature is greater than that of the lower portion. In figure 3, we represent an illustration of the variation of the axial velocity in the exit of annulus (Z^*=217.39).

4.2 Development of temperature field

The angular distribution of the temperature field in the presence of eight longitudinal fins at the annulus exit is shown in figure 4. The maximum fluid temperature is equal to 0.5356 situated at the top of the annulus at r^*=1.0435, θ=0 and z^*=217.39. In this axial position, the minimum temperature of the fluid is in the lower part of annulus at θ = π and r^* = 0.6450. In figure 5, we represent the variation of the axial temperature at the end of each fin at r^*=0.8169. It is clear that the temperature of the vertical fin placed at θ=0 is highest, followed by fin placed at θ=π/4, π/2, 3π/4 and π.

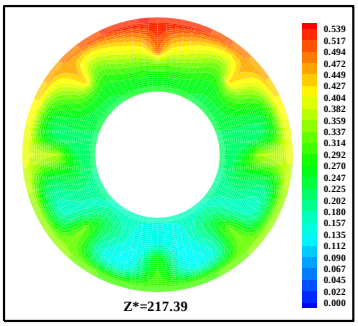

Figure 4 : Temperature field at the exit of annulus.

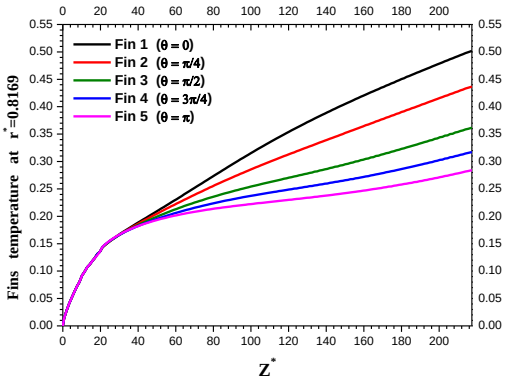

Figure 5 : Axial temperature variation of the fins at r^*=0.8169 .

4.3 Evolution of the axial local Nusselt number

The variation of the Nusselt number at the interface of the outer cylinder is illustrated in figure 6. The local Nusselt number at the interface (external pipe-fins) is zero. Apart from these azimuthal positions, the local Nusselt number takes a minimum value at the top of the cylindrical interface and a maximum value at the bottom of the cylindrical interface. At the exit of annulus, the local Nusselt number of the outer cylinder take a maximum value equal to 48.02 at θ=2.8203. The local Nusselt number of the longitudinal fin placed at (θ=π) is shown in Figure 7. This number take a maximum value equal to 130.00 at z^*=217.39 and r^*=0.8169.

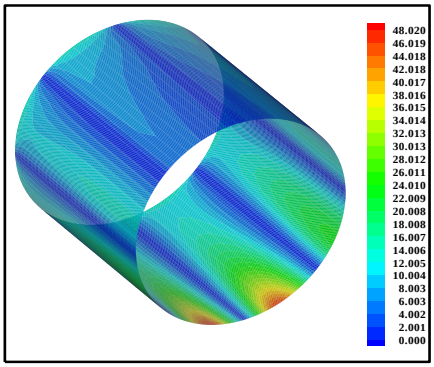

Figure 6: Evaluation of the local Nusselt number at the external cylinder interface

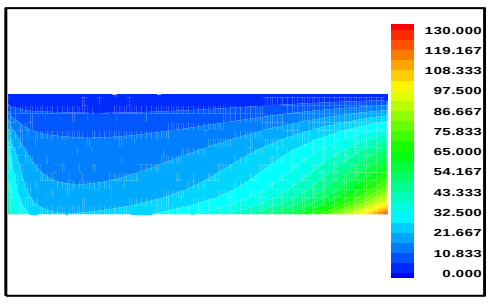

Figure 7: Evaluation of the local Nusselt number at the fin interface located at (θ=π).

Conclusion

This study considers the numerical simulation of the three dimensional mixed convection heat transfer in annulus equipped by longitudinal fins. The pipe and the fins are heated by an electrical current passing through its small thickness. The results show that the increase in the number of fins increases the axial Nusselt number especially when the flow is fully developed. The increase in the height of the fin from 0.12 to 0.24 improves the average Nusselt number from 41.89 to 60.09 in cases of eight fins. In this case, the maximum heat rate transferred to the fluid, is equal to 4.039, and is positioned on the fin located at (θ=0, z^*=93.07) while the maximum Nusselt number equal to 130.00 is positioned on the fin located at (θ=π, z^*=217.39).

Nomenclature

D_{1i} internal diameter of inner pipe, *m*
D_{1o} external diameter of inner pipe, *m*
D_{2i} internal diameter of outer pipe, *m*
D_{2o} external diameter of outer pipe, *m*
L annulus length, *m*
H fin height, *m*
g gravitational acceleration, $=9.81 m/s^2$
G volumetric heat generation, W/m^3
Gr^* modified Grashof number, $\left(g \beta G D_h^5 / K_s \nu^2\right)$
h_r radiative heat transfer coefficient, W/m^2K
h_c convective heat transfer coefficient, W/m^2K
K^* non dimensional thermal conductivity, K/K_0
K_s pipe thermal conductivity, *W/m K*
$Nu\ (\theta, Z^*)$ local Nusselt number.
P^* non-dimensional pressure, $\left(P - P_0\right) / \rho_0 V_0^2$.
Pr Prandtl number, ν/α
r^* non-dimensional radial coordinate, r / D_h.
Re Reynolds number, $V_0 D_h / \nu_0$
t^* non-dimensional time, $V_0 t / D_h$
T^* non-dimensional Temperature, $\left(T - T_0\right) / \left(G D_h^2 / K_s\right)$
V_0 average axial velocity at the entrance, *m/s*
V^* non-dimensional velocity, V^* / V_0
z^* non-dimensional axial coordinate, z / D_h

Greek Symbols
α thermal diffusivity, m^2/s
β thermal expansion coefficient, *(1/K)*
ε emissivity coefficient
θ angular coordinate, *rad*
μ dynamic viscosity, *kg m/s*
ν cinematic viscosity, m^2/s
τ^* non-dimensional stress, $\tau / \left(\mu_0 V_0 / D_i\right)$

References

[1] S.V. Patankar, M. Ivanovic and E.M. Sparrow, Analysis of Turbulent Flow and Heat Transfer in Internally Finned Tubes and Annuli, *J. Heat Transfer,* Volume 101, page 29-37, 1979.
[2] A.K. Agrawal and S. Sengupta, Laminar flow and Heat Transfer in a Finned Tube Annulus, *Int. J. Heat and Fluid Flow,* Volume 11(1), page 54-59, 1990.
[3] M.I. Farinas, A. Garon and K. Saint-Lous, Study of Heat Transfer in a Horizontal Cylinder with Fins, Revue *Générale de Thermique*, Volume 36, page 398-410, 1997.
[4] Wei-Mon Yan and Pay-Jen Sheen, Heat transfer and friction characteristics of fin and tube heat exchangers, *International Journal of Heat and Mass Transfer,* Volume 43, page 1651–1659, 2000.
[5] B. Yu, J.H. Nie, Q.W. Wang and W.Q. Tao, Experimental study on the pressure drop and heat transfer characteristics of tubes with internal longitudinal fins, *Heat and Mass Transfer,* Volume 35, page 65-73, 1999.
[6] C.C. Wang, W.L. Fu and C.T. Chang, Heat transfer and friction characteristics of typical wavy fin and tube heat exchanger, *Exper. Thermal Fluid Science,* Volume 14, page 174 – 186, 1997.
[7] H.D. Baehr and K. Stephan, *Heat and Mass Transfer,* Springer- Verlag, Berlin, 1998.
[8] S.W. Churchill and H.S. Chu, Correlating Equation for Laminar and Turbulent Free Convection from a Horizontal Cylinder, *International Journal of Heat and Mass Transfer,* Volume 18, page 1049–1053, 1975.
[9] S. Patankar, *Numerical Heat Transfer and Fluid Flow,* McGraw-Hill, New-York, 1980.